第 31卷第 11期　　焊　接　学　报　　Vol.31　No.11
2010年 11月　　TRANSACTIONS OF THE CHINA WELDING INSTITUTION　　November　2010

低合金高强钢激光—电弧复合热源焊接冷裂纹敏感性分析

滕　彬，　李小宇，　雷　振，　王旭友
(机械科学研究院哈尔滨焊接研究所，哈尔滨　150080)

摘　要：通过扩散氢含量测定，并利用经验公式计算 JFE980S低合金高强钢冷裂纹敏感性和焊前预热温度，同时采用斜 Y形坡口试验、金相试验以及残余应力测定等方法，研究低合金高强钢抗冷裂性能，对比分析了激光—电弧复合焊和 MAG焊工艺对接头抗冷裂性能的影响。结果表明，激光复合焊抗冷裂性优于 MAG焊方法。因复合焊加入了激光，使得焊缝熔深增加，拘束减小，并且激光在前，对焊接试板有一定的预热作用，使冷裂纹形成倾向进一步降低，特别是在无法预热的情况下，激光复合焊更能够体现出优势。

关键词：高强钢；激光；复合热源焊接；冷裂纹
中图分类号：TG115.28　　文献标识码：A　　文章编号：0253-360X(2010)11-0061-04

滕　彬

0　序　　言

低合金调质高强钢是最具发展前景的一种高强钢，此钢种因具有优异的综合性能和良好的经济效益，多用于重要的焊接结构，在建筑、桥梁、船舶、石油化工、工程机械、压力容器、海洋工程、核能等重要工业领域得到了广泛的应用。低合金高强度钢焊接中易产生冷裂纹，冷裂纹的产生主要是由淬硬组织、氢的富集和拘束应力三要素共同作用的结果[1]。

对于低合金高强钢的焊接，国内外的研究多集中于一些常规的焊接方法。激光—电弧复合热源焊是 20世纪 70年代出现的一种新兴焊接方法，随着该方法的发展，激光—电弧焊已在很多领域得到了应用。对于此方面的研究多集中在工艺基础方面，对其焊接性的研究相对较少。因此作者采用激光—电弧复合热源对 JFE980S和 HG980D低合金高强钢焊接冷裂纹敏感性方面进行研究，并与常规 MAG焊对比，分析两种焊接方法的冷裂纹敏感程度、合理的预热温度，具有重要的工程意义。

1　试验方法

试验所用低合金调质高强钢材质为 JFE980S和 HG980D，钢板厚度分别为 12，25 mm；焊材为 ϕ1.2 HS-80焊丝；激光器为额定功率 2 kW的连续波 Nd：YAG激光器，试验中采用焦距为 200 mm的激光输出透镜；MAG/MIG焊所用设备为 TPS5000型数字化电源。母材力学性能见表 1，母材及焊丝的化学成分见表 2。试验通过对焊接冷裂纹敏感指数、斜 Y形坡口焊接裂纹试验、焊接残余应力测定试验等分析方法，对激光—电弧复合热源焊接方法和常规

表 1　JFE980S和 HG980D钢板力学性能
Table 1　Properties of JFE980S and HG980D

	屈服强度 R_{eL}/MPa	抗拉强度 R_m/MPa	断后伸长率 A(%)	冲击吸收功 $A_{KV(-20℃)}$/J
JFE980S	960	1 005	12.6	>47
HG980D	940	970	17.0	>30

表 2　JFE980S和 HG980D钢及焊丝化学成分(质量分数，%)
Table 2　Chemical composition of JFE980S and HG980D and wire

	C	Si	Mn	S	P	Cr
JFE980S	0.14	0.25	0.92	<0.01	<0.01	0.62
HG980D	0.10	0.30	1.43	<0.01	0.01	0.48
HS-80	0.09	0.55	1.68	<0.01	<0.01	0.02
	Ni	Mo	Ti	V	Nb	Fe
JFE980S	0.03	0.16	0.01	0.04	<0.001	余量
HG980D	0.61	0.41	—	—	<0.001	余量
HS-80	1.02	0.43	0.09	—	—	余量

收稿日期：2009-07-27
基金项目：国家“十一五”科技支撑计划资助项目（2006BAF04B10）

MAG焊接方法在抵抗冷裂纹敏感性方面进行分析[2,3].

2 焊接冷裂纹敏感性评定

2.1 焊接冷裂纹敏感指数

在评价冷裂纹敏感性方面,日本的伊藤等人建立了焊接冷裂纹敏感指数 P_{cm}经验公式,并通过焊接冷裂纹敏感指数 P_{cm}、板厚 h、扩散氢含量等参量得出冷裂纹敏感性 P_W公式及防止冷裂纹所需的焊前预热温度 T_0的计算公式[4,5]为

$$P_{cm} = C + Si/30 + (Mn + Cu + Cr)/20 + Ni/60 + Mo/15 + V/10 + 5B \quad (1)$$

$$P_W = P_{cm} + [H]/60 + h/600 \quad (2)$$

$$T_0 = 1\,440 P_W - 392 \quad (3)$$

式中:[H]为熔敷金属中扩散氢含量.

扩散氢含量测定按照国家标准 GB/T3965—1995执行,利用气相色谱法测得的激光复合焊JFE980S高强钢扩散氢含量为 2.3 mL/100 g,常规焊为 3.3 mL/100 g,两种方法测得的扩散氢含量均在超低氢范围之内,并且激光复合焊扩散氢含量小于常规 MAG焊,利用 P_W 和预热温度经验公式进行计算,常规焊和激光复合焊的 P_W分别为 0.316%和 0.299%,通过式(3)计算出两种方法相应的预热温度 T_0分别为 63,39 ℃,因此,激光复合焊冷裂纹敏感性比常规 MAG焊低.

2.2 斜 Y形坡口焊接裂纹试验

斜 Y形坡口裂纹试验依据国家标准 GB4675.1—1984进行.试板尺寸见图 1.焊前用烘干炉对焊接试板进行 150 ℃×2 h烘干.由于钢板厚度不同,焊接结构的拘束程度不同,因此,试验对 12 mm厚的JFE980S高强钢和 25 mm厚 HG980D低合金高强钢进行了斜 Y形坡口裂纹试验.表 3为 JFE980S钢斜Y形坡口试验焊接工艺参数及试验结果,表 4为HG980D钢试验焊接工艺参数及试验结果.图 2为JFE980S钢在两种焊接工艺下宏观断面裂纹形貌.

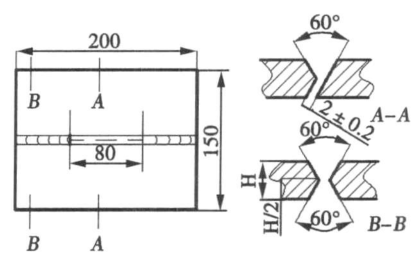

图 1 斜 Y形坡口焊接裂纹试板示意图(mm)
Fig.1 Size of specimen of slit type cracking test

表 3 JFE980S钢斜 Y形坡口试验焊接工艺参数及试验结果
Table 3 Welding parameters of JFE980S and results of slit type cracking test

编号	电流 I/A	电压 U/V	焊接速度 v/(mm·min⁻¹)	激光功率 P/W	预热温度 T_0/℃	表面裂纹率(%)	断面裂纹率(%)
1	214	27.0	500	1 500	无	0	0
2	213	26.4	500	—	无	0	100
3	215	26.7	500	—	60	0	0
4	249	27.8	800	1 500	无	0	0

表 4 HG980D钢斜 Y形坡口试验焊接工艺参数及试验结果
Table 4 Welding parameters of HG980D and results of slit type cracking test

编号	电流 I/A	电压 U/V	焊接速度 v/(mm·min⁻¹)	激光功率 P/W	预热温度 T_0/℃	表面裂纹率(%)	断面裂纹率(%)
1	245	26.5	500	2 000	无	100	80
2	245	26.5	500	2 000	60	0	0
3	260	28.0	500	—	60	60	80
4	260	28.0	420	—	100	0	0

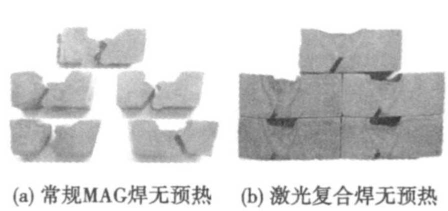

图 2 JFE980S斜 Y形坡口断面裂纹形貌
Fig.2 Photo of slit type cracking test of JFE980S

从表 3及图 2可知,12 mm厚 JFE980S激光复合方法和常规 MAG焊方法在采用相同的焊接工艺参数时(1号、2号、3号),激光复合方法在不预热情况下仍没有裂纹产生,而常规 MAG焊在无预热情况断面裂纹率达到 100%,当预热温度提高到 60 ℃时,裂纹消除.激光复合焊具有焊接效率高、焊接速度快的特点,当焊接速度提高到 800 mm/min时,对

激光复合焊方法进行了试验，结果发现在无预热情况下仍没有裂纹的产生．对 25 mm厚 HG980D钢进行试验时，常规 MAG焊预热温度达到 100 ℃无裂纹，而采用激光复合焊时预热温度只需要 60 ℃．因此，采用激光复合方法焊接高强钢时，接头抗冷裂纹性较好，这与经验公式推算结果一致．由于采用激光复合焊时，激光在前，电弧在后的焊接工艺，激光首先照射到焊接试板，使激光光斑附近区域的焊接试板局部温度升高，在一定程度上起到了提前预热的作用．另外，激光的加入，使周围区域的金属熔化，并与电弧共同作用下，熔深增加，拘束应力降低．

2.3　残余应力测试

残余应力是冷裂纹形成原因之一．通过采用压痕法试验方法对试板堆焊焊道表面残余应力进行了测量，来评价两种焊接方法的残余应力值分布规律．测量点位置分布如图 3所示．

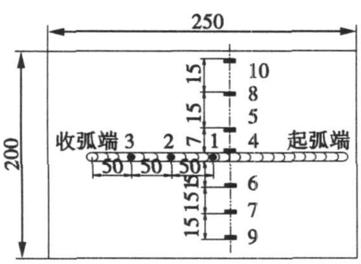

图 3　试板应力检测位置（mm）
Fig. 3　Location of measuring stress in plate

图 4为常规 MAG焊和激光复合焊焊缝中心区域纵向应力分布，检测位置如图 3中 1点、2点、3点．两种方法下的焊接电流均为 270 A，电压均为 30 V，常规焊和激光复合焊的焊接速度分别为 0.33 m/min和 0.80 m/min，激光功率为 1 500 W．从图 4中可以发现，常规 MAG焊焊缝中心残余应力高于激光复合焊残余应力，是激光复合焊的 2倍．从前面斜 Y形坡口裂纹试验的宏观形貌发现，裂纹主要在焊缝根部起裂，并沿焊缝中心部位断裂，除焊缝根部外，焊缝处是裂纹扩展的薄弱环节．因此，由于采用激光复合焊工艺，焊缝处残余应力偏低，从而提高了材料接头的抗冷裂性能．

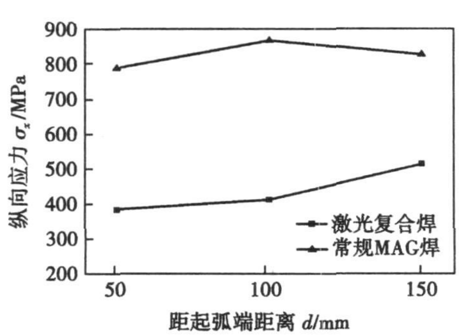

图 4　焊缝中心处纵向应力分布
Fig. 4　Longitudinal distribution of stress in weld center

图 5分别为垂直焊缝处纵向、横向应力分布，检测位置为图 3中 1点、4点 ~10点．

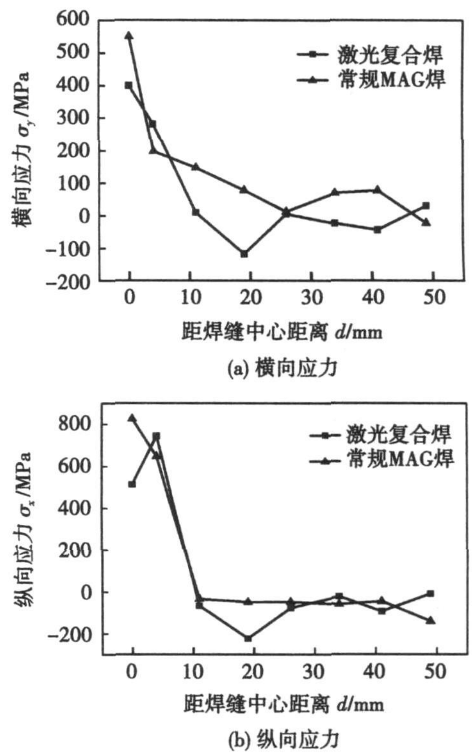

图 5　垂直焊缝应力分布
Fig. 5　Distribution of stress in vertical weld

从图 5中可知两种焊接方法的纵向残余应力均较高，常规 MAG焊和激光复合焊应力分别为母材屈服强度的 0.87倍和 0.78倍．两种焊接方法的拉伸应力区宽度单边均达到 10 mm，两种焊接方法的横向残余应力分布规律有一定差别．常规 MAG焊的焊缝应力高，达到母材屈服强度的 0.57倍，且拉压力区宽度较宽，单边超过 40 mm．而复合焊的拉压力区宽度仅为 10 mm左右，焊缝最大应力数值也比常规焊低．综上所述，与常规 MAG焊相比，激光复合焊残余应力偏低．

2.4　组织分析

低合金高强度钢焊接热影响区主要组织类型为马氏体（M，ML）、贝氏体（B_U，B_L，BL）和 F+P，当热影响区为 ML+BI组织时韧性最好，强度最高，随着 B_U组织的增加韧性急剧下降．热影响区韧性除与组织类型有关外，还与晶粒度有很大关系．从快冷

时的 MI组织向慢冷时的 F+ B_s组织变化时,脆性转变温度(vT_{rs})与有效晶粒尺寸 $d_e^{-1/2}$ 有线性关系,晶粒尺寸 d_e越小, vT_{rs}越低[1]. 图 6为激光复合焊和常规 MAG焊金相组织形貌. 由图 6可见,两种方法下焊缝组织相同,均为粒状贝氏体组织;常规 MAG焊粗晶区组织为粒状贝氏体+板条马氏体,其中粒状贝氏体占多数,晶粒度为 3. 5级,粗晶区宽度为 0. 5 mm;而激光复合焊粗晶区组织为板条马氏体+粒状贝氏体,以板条马氏体为主,晶粒度为 4级,粗晶区宽度为 0. 4 mm. 尽管两种焊接方法下焊缝组织相同,但在热影响区处激光复合焊获得的板条马氏体组织综合性能优越,而且晶粒细小,导致激光复合焊在抑制冷裂纹上有一定的优势.

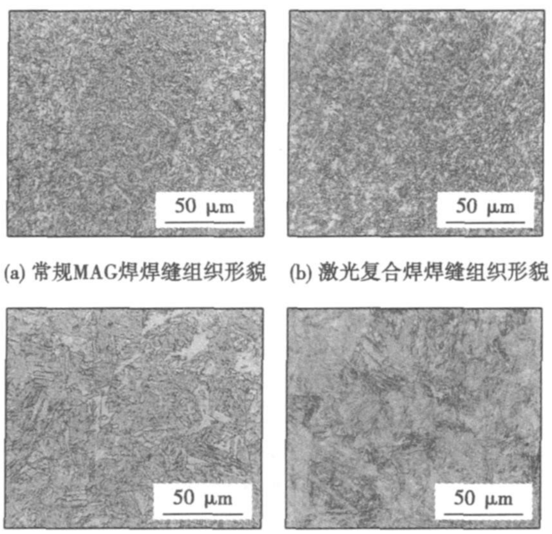

(a) 常规MAG焊焊缝组织形貌 (b) 激光复合焊焊缝组织形貌

(c) 常规MAG焊粗晶区组织形貌 (d)激光复合焊粗晶区组织形貌

图 6 焊缝及粗晶区组织形貌

Fig. 6 Microstructure of weld and coarse grain zone

3 结 论

(1)激光复合焊冷裂纹敏感性和预热温度均低于 MAG焊.

(2)对于 12 mm厚 JFE980S钢,激光-电弧复合热源焊接方法不需要预热,常规 MAG焊需预热 60 ℃;对于 25 mm厚 HG980D钢激光-电弧复合热源焊接方法需预热 60 ℃,常规 MAG焊需预热 100 ℃.

(3)激光复合焊扩散氢含量和残余应力水平均低于常规 MAG焊,抗冷裂性优于常规 MAG焊.

(4)与常规 MAG焊对比,激光复合焊获得的组织更加细小,粗晶区宽度更窄.

参考文献:

[1] 邹增大,李亚江,尹士科. 低合金调质高强度钢焊接及工程应用[M]. 北京:化学工业出版社, 2003

[2] 窦万波. 10 000 m³ 天然气球罐用 WEL-TEN610CF焊接冷裂纹敏感性[J]. 石油化工设备, 2007, 36(3): 8-11.
Dou Wanbo. Synthetic evaluation to cold crack sensitivity of WEL-TEN610CF steel used in 10 000 m³ natural gas spherical tank[J]. Petro-Chemical Equipment, 2007, 36(3): 8-11.

[3] 杜 义,张田宏,张俊旭. 10Ni8CrMoV钢的冷裂纹敏感性分析[J]. 焊接学报, 2006, 27(12): 93-96.
Du Yi, Zhang Tianhong, Zhang Junxu. Analysis on welding cold crack sensibility of 10Ni8CrMoV steel[J]. Transactions of the China Welding Institution, 2006, 27(12): 93-96.

[4] 曹良裕, 魏战江. 钢的碳当量公式及其在焊接中的应用[J]. 材料开发与应用, 1999, 14(1): 39-43.
Cao Liangyu, Wei Zhanjiang. The carbon equivalent formula of steel and its application in the welding[J]. Development and Application of Materials, 1999, 14(1): 39-43.

[5] 王晓香. 管线钢焊接常用的几种碳当量公式[J]. 焊管, 2004, 27(2): 71-76.
Wang Xiaoxiang. Several carbon equivalent calculation commonly applied into linepipe weld[J]. Welding Pipeline, 2004, 27(2): 71-76.

作者简介:滕 彬,男, 1982年出生,硕士. 主要从事激光加工和激光-电弧复合热源焊接技术方面研究. 发表论文 1篇.
Email: tengbin134@163.com

Tianjin University, Tianjin 300072, China; 2. Qinhuangdao Institute of Measurement and Testing Technology, Qinhuangdao 066000, Hebei, China). p 57－60

Abstract: In order to improve the fatigue performance of Ti alloy welded joints, the weld toe in cross-shaped joint was processed by the HJ-II type ultrasonic peening treat plant developed by authors. The test results indicate that when the stress ratio R is equal to 0.5 in loading condition, the conventional ultrasonic peening processing makes the fatigue strength of the cross-shaped joint of TC4 titanium alloy be enhanced by about 73.5%, the life be lengthened about 12－17 times, while loading ultrasonic peening processing makes the fatigue strength of the cross shaped joint of TC4 titanium alloy be enhanced by about 148.1%, and the life be lengthened about 23－26 times. Meanwhile, the mechanism for the fatigue performance of welded joints enhanced by the ultrasonic peening, especially the loading ultrasonic peening, is expounded from the change of the stress concentration factor after the ultrasonic peening, the change of the residual stress of welded joints, the plastic deformation in the surface layer of the weld toe area and the change in hardness.

Key words: welded joint; fatigue performance; loading ultrasonic peening

Analysis on cold crack sensitivity of low alloy high strength steel weld by laser-arc hybrid welding

TENG Bin, LI Xiaoyu, LEI Zhen, WANG Xuyou (Harbin Welding Institute, China Academy of Machinery Science & Technology, Harbin 150080, China). p 61－64

Abstract: The preheating temperature and cold crack sensitivity of low alloy high strength steel JFE980S were calculated according to the empirical formula and the measured diffusible hydrogen content. By the Y-slit type cracking test, the metallographic test, and the residual stresses measurement, the cold crack resistance of the low alloy high strength steel joint were analyzed and compared between the laser-arc hybrid welding and the MAG welding. The results show that the steel welded by laser-arc hybrid welding has smaller cold crack tendency than that by the MAG welding because of the higher weld penetration and the decreases in the welding stress. The laser can preheat the base metal when the laser is ahead of the MAG arc, and the steel has lower welding residual stresses. Laser-arc hybrid welding has an advantage over the MAG welding without non-preheating welding for JFE980S high strength steel.

Key words: high strength steel; laser; hybrid welding; cold crack

Effect of boron carbide on properties of arc spraying coatings

WEI Qi, GAO Ming, LI Hui, LU Lanzhi (College of Materials Science and Engineering, Beijing University of Technology, Beijing 100124, China). p 65－68

Abstract: A cored wire containing the boron carbide ceramic powder and other alloying elements powder was fabricated with 304L stainless steel sheath and the metal ceramic composite coating was deposited by arc spraying. The feasibility of boron carbide in the application of arc spraying was studied. The microstructure, phase compositions and worn surface morphologies of the coatings were analyzed by means of scanning electron microscopy and X-ray diffraction. High temperature abrasive wear performance and erosion performance were evaluated by high-temperature abrasive wear tester designed by authors and high temperature erosion devices, respectively. The results show that the cored wires have good process ability for arc spraying. The composite coatings contains Fe_3B, CrB, $FexNi_{23-x}B_6$, $Fe_{23}(C,B)_6$, $(Cr,Fe)_7C_3$ and Fe_3C hard phases due to the in-situ synthesis of B_4C ceramic particle with other alloying elements powder, which result in a significant increase in the hardness, wear resistantance and erosion-resistantance of the coating.

Key words: boron carbide; wear; arc spraying; cored wire

Effect of aging treatment on microstructure of 2205 duplex stainless steel welds

ZOU Dening, HAN Ying[1,3], FAN Guangwei[1,3], ZHANG Wei[2] (1. School of Metallurgy and Engineering, Xi'an University of Architecture and Technology, Xi'an 710055, China; 2. State Key Laboratory of Advanced Stainless Steel Materials, Taigang Stainless Steel Co., Ltd., Taiyuan 030003, China; 3. State Key Laboratory for Mechanical Behavior of Metal Materials, Xi'an Jiao Tong University, Xi'an 710049, China). p 69－72

Abstract: The solution-treated welded joints of 2205 duplex stainless steel welded by shielded metal arc welding were treated by aging treatment at 850 ℃ for 30, 180 and 360 min, respectively. The microstructure evolution and the precipitation of σ phase were analyzed by OM, XRD, EDS and ferrite scope detector. The results indicate that in each region of the aged joints, σ phase precipitates at γ/α or α/α grain boundaries and grows into ferrite phase. The formation mechanism is a eutectoid reaction of $\alpha \rightarrow \sigma + \gamma_2$. The increase of aging time leads to a decrease in ferrite phase and an increase in σ phase. σ phase morphology changes from spotted→reticular→schistic state. Compared to the base metal and HAZ, the weld metal with the most precipitation rate of σ phase is more sensitive to the aging treatment, in which the ferrite almost completely transforms into austenite and σ phase after aging for 360 min.

Key words: duplex stainless steel; welded joint; solution treatment; aging; microstructure

Abrasive wear behavior of Fe-Cr-C hardfacing alloy

WANG Zhihui, HE Dingyong, JIANG Jianmin, CUI Li (School of Materials Science and Engineering, Beijing University of Technology, Beijing 100124, China). p 73－76

Abstract: Fe-Cr-C abrasive wear resistant layers were prepared on Q235 steel by submerged arc welding. The abrasive wear resistance of the layers was evaluated by an MLS-225 grain abrasion test machine. The abrasive wear mechanism was studied according to the analysis on of surface topography by the micro examination and energy spectrum analysis. The results indicated the wear mechanism of Fe-Cr-C abrasive wear resistant layer was mainly attributed to the exfoliation caused by micro crack. The desquamation was closely correlated with the carbide. Energy spectrum analysis indicated that the Cr content in the crater-like pits was inosculated with the Cr content in $(Cr,Fe)_7C_3$, which